ZEBRAFISH
Volume 11, Number 6, 2014

DOI: 10.1089/zeb.2014.1024

The Tumor Suppressor *rpl36* Restrains KRAS^{G12V}-Induced Pancreatic Cancer

Elayne Provost,[1,*] Jennifer M. Bailey,[1,2,*] Sumar Aldrugh,[3] Shu Liu,[1] Christine Iacobuzio-Donahue,[2] and Steven D. Leach[1,4,†]

Abstract

Ribosomal proteins are known to be required for proper assembly of mature ribosomes. Recent studies indicate an additional role for ribosomal proteins as candidate tumor suppressor genes. Pancreatic acinar cells, recently identified as effective cells of origin for pancreatic adenocarcinoma, display especially high-level expression of multiple ribosomal proteins. We, therefore, functionally interrogated the ability of two ribosomal proteins, *rpl36* and *rpl23a*, to alter the response to oncogenic Kras in pancreatic acinar cells using a newly established model of zebrafish pancreatic cancer. These studies reveal that *rpl36*, but not *rpl23a,* acts as a haploinsufficient tumor suppressor, as manifested by more rapid tumor progression and decreased survival in *rpl36$^{hi1807/+}$;ptf1a:gal4VP16^{Tg};UAS:GFP-KRAS^{G12V}* fish compared with their *rpl36$^{+/+}$;ptf1a:gal4VP16;UAS:GFP-KRAS^{G12V}* siblings. These results suggest that *rpl36* may function as an effective tumor suppressor during pancreatic tumorigenesis.

Introduction

Pancreatic cancer remains one of the deadliest forms of cancer, with dismal patient survival rates observed even for early-stage disease. *KRAS* is the most frequently mutated gene in pancreatic cancer and activates a number of signaling pathways that together promote the initiation of pancreatic intraepithelial neoplasia (PanIN) and eventual progression to pancreatic cancer.[1] Despite the high frequency of *KRAS* mutations and recent advances in animal modeling, the identification of additional genetic and epigenetic changes that either accelerate or restrain *KRAS*-driven pancreatic neoplasia remains an area of critical investigation and discovery.[2]

Ribosomal protein large subunit (Rpl) genes are highly expressed in both the developing endoderm and adult endoderm-derived tissues.[3] In addition to known roles in ribosome assembly, recent experiments in zebrafish have shown that a select group of ribosomal proteins may also function as effective tumor suppressor genes. In a large-scale zebrafish insertional mutagenesis screen, mutations in 28 different ribosomal proteins were identified, all with embryonic lethal homozygous phenotypes.[4] For 17 of these mutations, adult heterozygotes displayed high rates of malignant peripheral nerve sheath tumors (zMPNST), well above the rate observed within the larger population of fish bearing retroviral insertions.[5,6] Among the genes identified as haploinsufficient tumor suppressors were rpl23a and rpl36.[6] Human RPL23a has previously been shown to modify the malignant phenotype of gastric cancer cells through interactions with MDM-2 and p53, while RPL36 has been implicated in mediating resistance of cancer cells to cisplatin.[7,8]

Recently, phosphorylation of ribosomal protein S6 was identified as a critical regulator of Kras-mediated PanIN progression in a murine model of pancreatic cancer.[9] However, the role of other ribosomal proteins in modulating cellular responses to oncogenic Kras has not been well defined. Thus, we sought to determine whether haplo-insufficiency for *rpl23a* or *rpl36* might modify the response to oncogenic Kras in a zebrafish model of pancreatic tumorigenesis. We used a novel zebrafish model (here denoted as KG^{ptf1a}) in which expression of a UAS-regulated GFP-KRAS^{G12V} fusion[10] is activated by Gal4/VP16[11] under the control of *ptf1a* regulatory elements. In this model, human oncogenic KRAS is expressed in early pancreatic progenitor cells within the developing pancreas, as well as in adult acinar cells. Using this system, we show that *rpl36* restrains Kras-driven pancreatic tumorigenesis. Zebrafish expressing GFP-KRAS^{G12V} in the setting of *rpl36* haploinsufficiency demonstrated increased pancreatic epithelial cell proliferation, significantly accelerated tumor progression, and decreased survival relative to *rpl36$^{+/+}$* sibling controls. In contrast, haploinsufficiency for *rpl23a* had no effect.

Departments of [1]Surgery and [2]Pathology, Johns Hopkins University, Baltimore, Maryland.
[3]Department of Medicine, Georgia Health Sciences University, Athens, Georgia.
[4]McKusick-Nathans Institute for Genetic Medicine, Johns Hopkins University, Baltimore, Maryland.
*These authors contributed equally to this work.
†Current affiliation: Memorial-Sloan Kettering Cancer Center, New York, New York.

Complementing these zebrafish studies, we also observed a progressive decrease in rpl36 expression human pancreatic cancer specimens and cell lines, as well as a reduction in rpl36 staining in a murine model of PanIN. Our data implicate *rpl36* as an apparent haploinsufficient tumor suppressor in vertebrate pancreas.

Materials and Methods

Fish strains and genotyping

All fish were raised using standard husbandry procedures approved by our institutional animal care and use committee. Fish were sacrificed either according to predefined time-points or as required due to gross abdominal distention and disrupted swimming behavior. The following fish strains were used in this study: Tg(BAC ptf1a:eGFP^{jh1}),[12] Tg(Tol2 ins:mCherry^{jh2}),[13] rpl23a^{hi2582} (obtained from ZIRC, Eugene, OR), rpl36^{hi1807} (obtained from ZIRC), Tg(BAC ptf1a:Gal4-VP16), and Tg(Tol2 UAS:GFP-KRAS^{G12V}).

Survival analysis

Kaplan–Meyer survival analysis was used to evaluate tumor incidence, time from tumor onset to death, and overall survival. Statistical comparisons were made using a log rank test, and data were analyzed using the Prism software package.

In situ *hybridization and immunofluorescent and labeling*

In situ hybridization for *rpl36* and *rpl23A* were performed as previously described.[3] Zebrafish were fixed overnight in 4% paraformaldehyde, processed, and embedded in paraffin. Paraffin-embedded tissue was serially cut into 5 μM sections. For experiments comparing tumor formation in *rpl36$^{hi1807/+}$;ptf1a:gal4VP16^{Tg};UAS:GFP-KRAS^{G12V}* (referred to as KG^{ptf1a};rpl36$^{hi1807/+}$) or *rpl23a$^{hi2582/+}$;ptf1a:gal4VP16^{Tg};UAS:GFP-KRAS^{G12V}* and *ptf1a:gal4VP16^{Tg};UAS:GFP-KRAS^{G12V}* (referred to as KG^{ptf1a};rpl23a$^{hi2582/+}$) siblings. The entire pancreas was sectioned and every fifth section was stained with hematoxylin and eosin, followed by histological examination.

Immunohistochemical labeling

For immunohistochemistry, RPL36 expression was analyzed on human tissue microarrays, including PanIN and invasive primary pancreatic ductal adenocarcinoma (PDAC). Sectioned arrays were rehydrated using histoclear and subjected to heat-mediated antigen retrieval (Vector). After antigen retrieval, the slides were washed in 1× PBS, permeabilized with 1% PBST (PBS-Tween-20). Rabbit anti-human RPL36 primary antibody (Novus 1:50) was diluted in 0.1%PBST and applied to sections overnight at 4°C. The slides were washed with 1× PBS and anti-rabbit secondary antibody and incubated at room temperature for 1 h before application of 3-3′-Diaminobenzidine tetrahydrochloride (DAB). The intensity of RPL36 expression in sections of normal human pancreas, chronic pancreatitis, and PanIN was scored on a scale from 0 to 3, with zero = no staining, 1 = light staining, 2 = moderate staining, and 3 = dark staining Two individual observers independently verified the staining intensity. The same method was used to score rpl36 expression in zebrafish tumors.

Fish strains & genotyping

Tail fins of adult fish, or individual larvae, were digested in low TE (10 mM Tris HCl 7.5, 1 mM EDTA) plus proteinase K at 55°C. PCR genotyping was done to confirm the retroviral insertion in the rpl23a^{hi2582} locus (forward primer 5′ CGAAGGCGAAGAAGGAAGGTG, reverse primer, 5′GT TCCTTGGGAGGGTCTCCTC), and the rpl36^{hi1807} locus (forward primer 5′ CTTAACCAGCGACGGCATGC, reverse primer, 5′GCTAGCTTGCCAAACCTACAGGT). PCR for the rpl23a WT allele confirmed the fidelity of the isolated DNA. Rpl23a^{WT} locus (forward primer 5′ CAGGCAATT GACACTTTGTTAG, reverse primer, 5′CAATTGTACGTG AACATGAAGG).

For each experiment, the following numbers of fish were utilized:

Survival (Fig. 4)

rpl23a$^{WT/WT}$;ptf1a:GAL4-VP16;UAS:GFP-KRAS^{G12V}
$n = 67$
rpl23a$^{2582/WT}$;ptf1a:GAL4-VP16;UAS:GFP-KRAS^{G12V}
$n = 34$
rpl36$^{WT/WT}$;ptf1a:GAL4-VP16;UAS:GFP-KRAS^{G12V}
$n = 29$
rpl36$^{hi1807/WT}$;ptf1a:GAL4-VP16;UAS:GFP-KRAS^{G12V}
$n = 26$

Timed Kill (Fig. 4)
3 month time point

rpl36$^{WT/WT}$;ptf1a:GAL4-VP16;UAS:GFP-KRAS^{G12V}
$n = 21$
rpl36$^{hi1807/WT}$;ptf1a:GAL4-VP16;UAS:GFP-KRAS^{G12V}
$n = 18$

7 month time point

rpl36$^{WT/WT}$;ptf1a:GAL4-VP16;UAS:GFP-KRAS^{G12V}
$n = 30$
rpl36$^{hi1807/WT}$;ptf1a:GAL4-VP16;UAS:GFP-KRAS^{G12V}
$n = 13$

Proliferation Quantification (Fig. 4)

rpl36$^{WT/WT}$;ptf1a:GAL4-VP16;UAS:GFP-KRAS^{G12V}
$n = 8$ fish, 18 sections
rpl36$^{hi1807/WT}$;ptf1a:GAL4-VP16;UAS:GFP-KRAS^{G12V}
$n = 8$, 15 sections

In situ *hybridization*

To perform *in situ* hybridization on paraffin sections, 12 μm sections were deparaffinized in histoclear and rehydrated. Sections were prehybridized (50% formamide, 5× SSC pH 4.5 w/citric acid, 50 μg/mL yeast tRNA, 1% SDS, and 50 μg/mL heparin) at 55°C for 2 h. Anti-sense *in situ* probes were boiled in prehybridization buffer (10 μL/mL), added to tissue sections, covered with a coverslip, and hybridized at 68°C in a humidity chamber overnight. Tissue sections were washed in 5× SSC at 68°C, followed by 0.2× SSC at 68 and Maelic acid buffer (MAB) at room temperature. Sections were blocked in 10% sheep serum diluted in MAB for 1 h and incubated with anti-digoxigenin alkaline phosphatase antibody at 1:5000 overnight at 4°C. Slides were washed with MAB + 0.1% Tween-20, and signal was detected using BM purple at room temperature. Reactions were

stopped with 1 mM EDTA pH8.0. Sense and antisense digoxigenin-labeled RNA probes were amplified for rpl23a (forward primer 5′ ATGGCCCCGAAGGCGAAG, reverse primer 5′ TTAGATGATGCCGATCTTGTTGGCAAC) and rpl36 (forward primer 5′ ATGGTTGTCAGATATCCTA TGGC, reverse primer 5′ CTACTCTTTCTTGGCAGCAG).

Microscopy

Live adult zebrafish were examined for subcutaneous tumor formation by first anesthetizing them with Tricaine and then examining them for GFP fluorescence on an SMZ1500 stereomicroscope (Nikon Instruments). Confocal imaging was done using UV, Argon, and He/Ne lasers for blue, green, and red channels, respectively, using a Nikon A1Rsi system.

Tumor sample collection and preparation

GFP-positive embryos were identified and raised from *rpl23a*$^{hi2582/WT}$*;ptf1a:GAL4-VP16* or *rpl36*$^{hi1807/WT}$*;ptf1a:GAL4-VP16* crossed to UAS:GFP-KRAS^{G12V} adult zebrafish. To evaluate for tumor latency, tumor progression, and overall survival, each month, adult zebrafish were anesthetized and examined for trans-abdominal GFP expression on a fluorescent stereomicroscope. When a tumor mass was identified, the fish was isolated and observed twice a week until the tumor filled the abdominal space and was interfering with swimming or feeding behaviors. Animals were then photographed, sacrificed, and the tumor and associated abdominal viscera were fixed in formalin for 24 h.

Immunofluorescent and immunohistochemical labeling for GFP and proliferating cell nuclear antigen

Paraffin-embedded 5 μM-thick sections of zebrafish pancreas were rehydrated using histoclear. Heat-mediated antigen retrieval was performed using Vector antigen retrieval solution. The tissues were permeabilized using 1% PBST and primary antibodies for detection of GFP and proliferating cell nuclear antigen (PCNA) (Santa Cruz) were diluted in 0.1% PBST and allowed to incubate overnight at 4°C. The next day, the slides were washed and species-specific secondary antibodies (anti-rabbit alexa-fluor 647 and anti-mouse alexa-fluor 488) were applied at room temperature for 1 h. Nuclei were stained using DAPI, and images were acquired using a Nikon

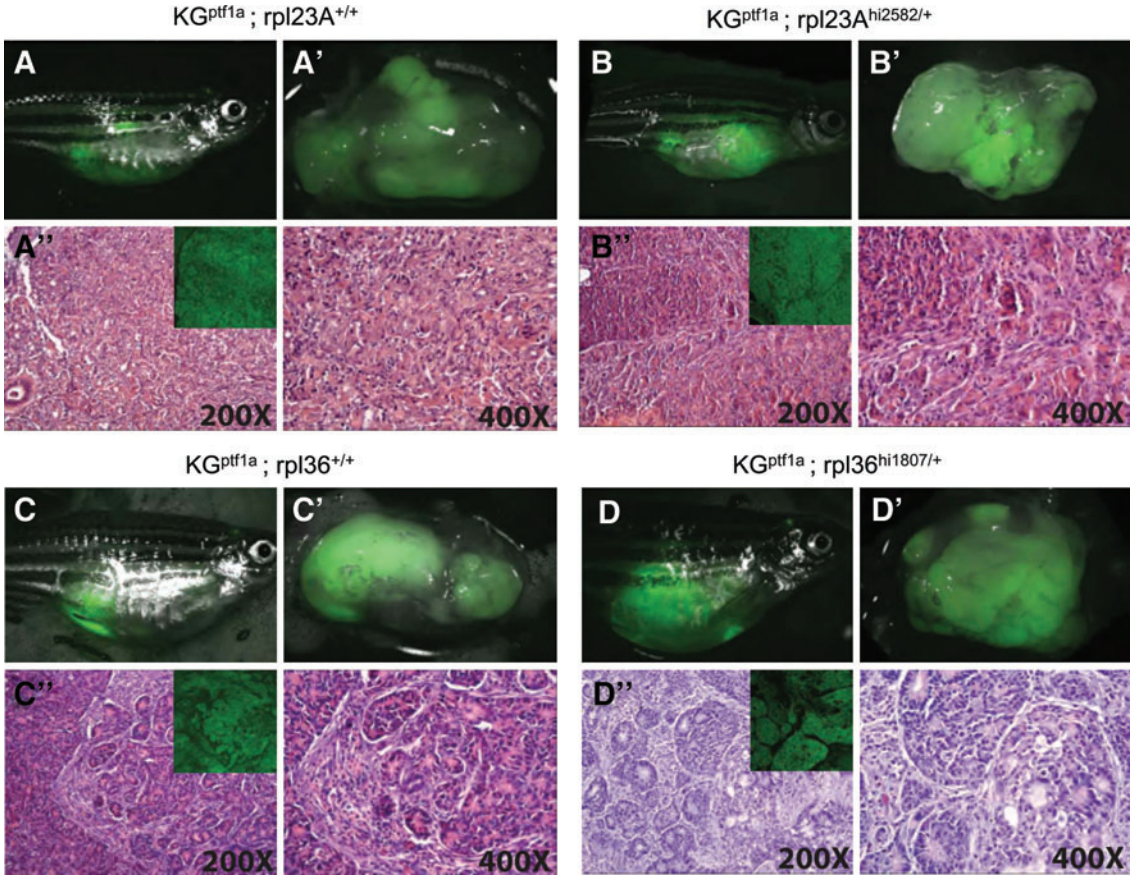

FIG. 1. Pancreatic tumor histology in the setting of haploinsufficiency for either rpl23a or rpl36. Representative images of 7-month-old *rpl23a*$^{WT/WT}$*; ptf1a:gal4-VP16; UAS:GFP-KRAS*^{G12V} **(A)**, *rpl23a*$^{hi2582/WT}$*; ptf1a:gal4-VP16; UAS:GFP-KRAS*^{G12V} **(B)**, *rpl36*$^{WT/WT}$*; ptf1a:gal4-VP16; UAS:GFP-KRAS*^{G12V} **(C)** and *rpl36*$^{hi1807/WT}$*; ptf1a:gal4-VP16; UAS:GFP-KRAS*^{G12V} fish **(D)**. For each genotype, *upper left* images depict fish with distended abdomen and transcutaneous eGFP fluorescence; *upper right* images depict excised abdominal viscera confirming eGFP + pancreatic tumors. *Lower panels* show representative histology of mixed acinar/ductal tumors. *Insets* confirm expression of GFP-KRAS^{G12V} fusion protein in malignant tumor epithelium as assessed by antibody staining for GFP (representative of $n = 96$ tumors analyzed). Color images available online at www.liebertpub.com/zeb

A1 confocal microscope. To quantify cell proliferation, the number of PCNA-positive pixels were determined using Nikon elements software, and normalized to total tumor area as determined by the total number of GFP-positive pixels.

Results

Rpl36 *and* rpl23a *are expressed in zebrafish pancreas, but their loss does not influence pancreatic development or tissue homeostasis*

In order to consider whether *rpl23a* and/or *rpl36* had the potential to influence pancreatic tumorigenesis, we first examined expression of these genes in adult zebrafish pancreas using *in situ* hybridization. These studies confirmed high-level expression in adult zebrafish pancreas and other endoderm-derived organs (Supplementary Fig. S1A, B). To determine whether haploinsufficiency for either of these genes altered normal pancreatic development and/or tissue homeostasis, the abdominal viscera of 7 month-old, tumor-free adult $rpl23a^{hi2582/+}$ and $rpl36^{hi1807/+}$ zebrafish were dissected for histological analysis. This revealed an entirely normal architecture of the exocrine and endocrine pancreas, as well as a histologically normal liver and intestine (Supplementary Fig. S1C, D).

Heterozygous loss of rpl36 *or* rpl23a *promotes nonpancreatic peripheral nerve sheath tumors*

As previously reported, aging $rpl23a^{hi2582}$ and $rpl36^{hi1807}$ heterozygotes displayed an increased incidence of zMPNSTs. We sectioned spontaneous tumors dissected from the abdomens of 15-month-old adult $rpl23a^{hi2582}$ and $rpl36^{hi1807}$ heterozygous zebrafish. These displayed the classic morphology of zMPNSTs and showed no expression of the pancreatic marker ptf1a:eGFP, confirming their nonpancreatic identity. (Supplementary Fig. S2C, D). In contrast to the rapid onset of pancreatic tumors induced by oncogenic KRAS (see Fig. 2), we observed no evidence of zMPNSTs in either line before one year of age. We also observed no change in pancreatic histology and no evidence of pancreatic tumors in either $rpl23a^{hi2582}$ or $rpl36^{hi1807}$ heterozygotes in the absence of oncogenic *KRAS* (Supplementary Fig. S2A, B).

Loss of rpl36 *accelerates* $KRAS^{G12D}$*-driven pancreatic cancer*

We next sought to determine whether haploinsufficiency for either *rpl23a* or *rpl36* might modify the response to oncogenic *KRAS*, the most frequently mutated gene in pancreatic cancer and a known initiator of pancreatic neoplasia.[14] $Rpl23a^{hi2582/+}$ and $rpl36^{hi1807/+}$ zebrafish were bred onto a

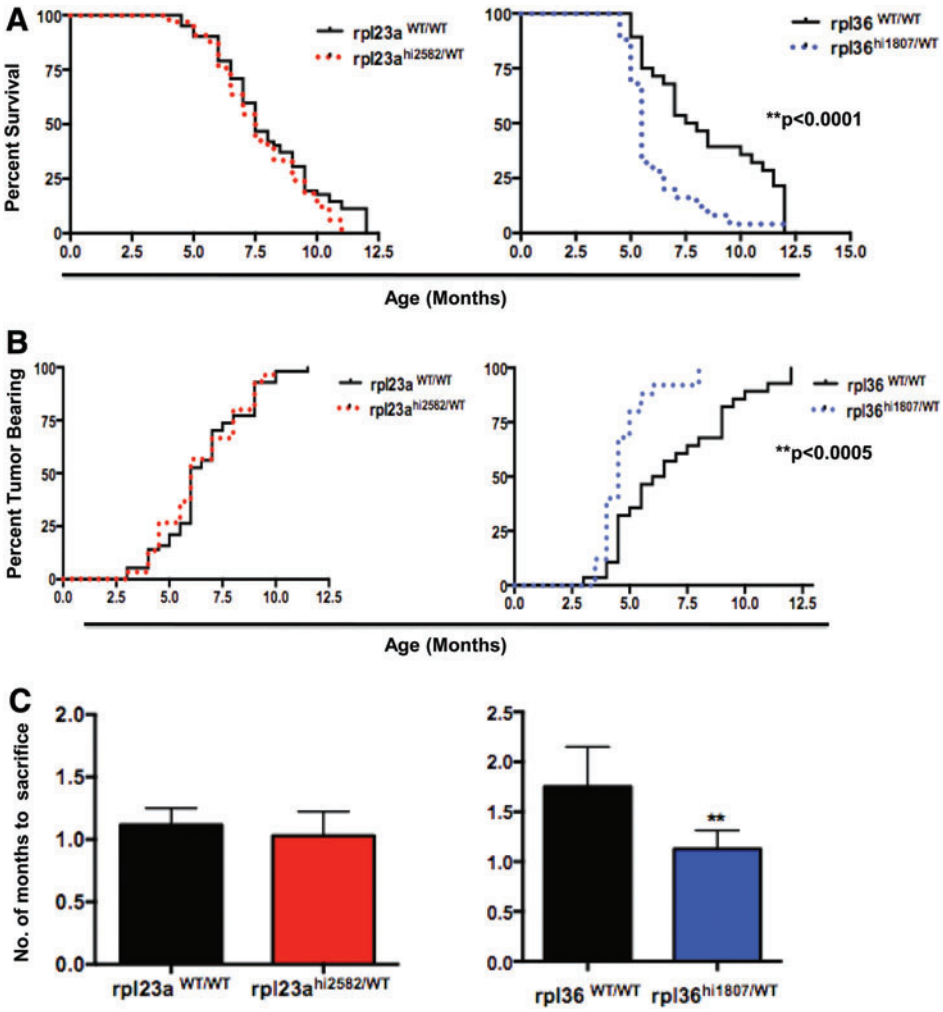

FIG. 2. Haploinsufficiency for *rpl36*, but not *rpl23a,* accelerates pancreatic tumorigenesis in ptf1a:Gal4-VP16; UAS:GFP-$KRAS^{G12V}$ transgenic zebrafish. **(A)** Age-dependent tumor incidence, **(B)** overall survival, and **(C)** time from tumor diagnosis to death for *ptf1a:Gal4-VP16; UAS:GFP-$KRAS^{G12V}$* (KG^{ptf1a}) fish with (*red*; $n=34$) and without (*black*; $n=67$) heterozygous *rpl23a* mutations and with (*blue*; $n=26$) and without (*black*; $n=29$) heterozygous *rpl36* mutations. $^{**}p<0.01$. Haploinsufficiency for *rpl23a* has no effect on tumor onset, tumor progression, or overall survival. In contrast, haploinsufficiency for *rpl36* accelerates tumor onset and tumor progression, and is associated with diminished overall survival. Color images available online at www.liebertpub.com/zeb

zebrafish pancreatic cancer model in which human oncogenic *KRAS*^{G12V} fused to eGFP is expressed under the regulation of UAS regulatory elements (*UAS:GFP-KRAS*^{G12V}).[15] In this system, UAS-driven expression of oncogenic KRAS is driven by chimeric Gal4/VP16 transcriptional activator incorporated into the ptf1a locus in a BAC transgene (*ptf1a:Gal4-VP16*),[16,17] resulting in expression in pancreatic progenitor cells as early as 34 h postfertilization (hpf), with ongoing expression in adult acinar cells. For simplicity, we refer to *UAS:GFP-KRASG12V; ptf1a:Gal4-VP16*^{Tg} fish as ''KG^{ptf1a}.''

Adult KG^{ptf1a} fish begin to develop pancreatic tumors between 2 and 3 months of age. Since the pancreatic tumor mass expands within the abdomen of these fish, GFP fluorescence can be observed transcutaneously in anesthetized living fish using a fluorescent dissecting microscope (Fig. 1). All KG^{ptf1a} fish shown in Figure 1 were sacrificed at 7 months of age and displayed large, *GFP-KRAS*^{G12V} expressing fluorescent tumors. We further confirmed expression of GFP in serial sections using an anti-GFP antibody to confirm the persistence of GFP-KRAS^{G12V} expression in tumors of all genotypes (Fig. 1A''–D'' insets). Expression of KG^{ptf1a} resulted in tumors of mixed acinar and ductal histology. No differences in tumor histology were observed in the presence or absence of mutations in either *rpl23a* (Fig. 1A–B'') or *rpl36* (Fig. 1C–D'').

In order to determine whether haploinsufficiency for either *rpl23a* or *rpl36* might affect pancreatic tumor incidence, progression, or overall survival, these features were compared in KG^{ptf1a} fish and their KG^{ptf1a}; rpl23a$^{hi2582/+}$ or KG^{ptf1a}; and rpl36$^{hi1807/+}$ mutant siblings. Haploinsufficiency for *rpl23a* had no effect on tumor incidence, tumor progression, or overall survival (Fig. 2A–C). In contrast, fish bearing a single *rpl36*^{hi1807} allele developed detectable

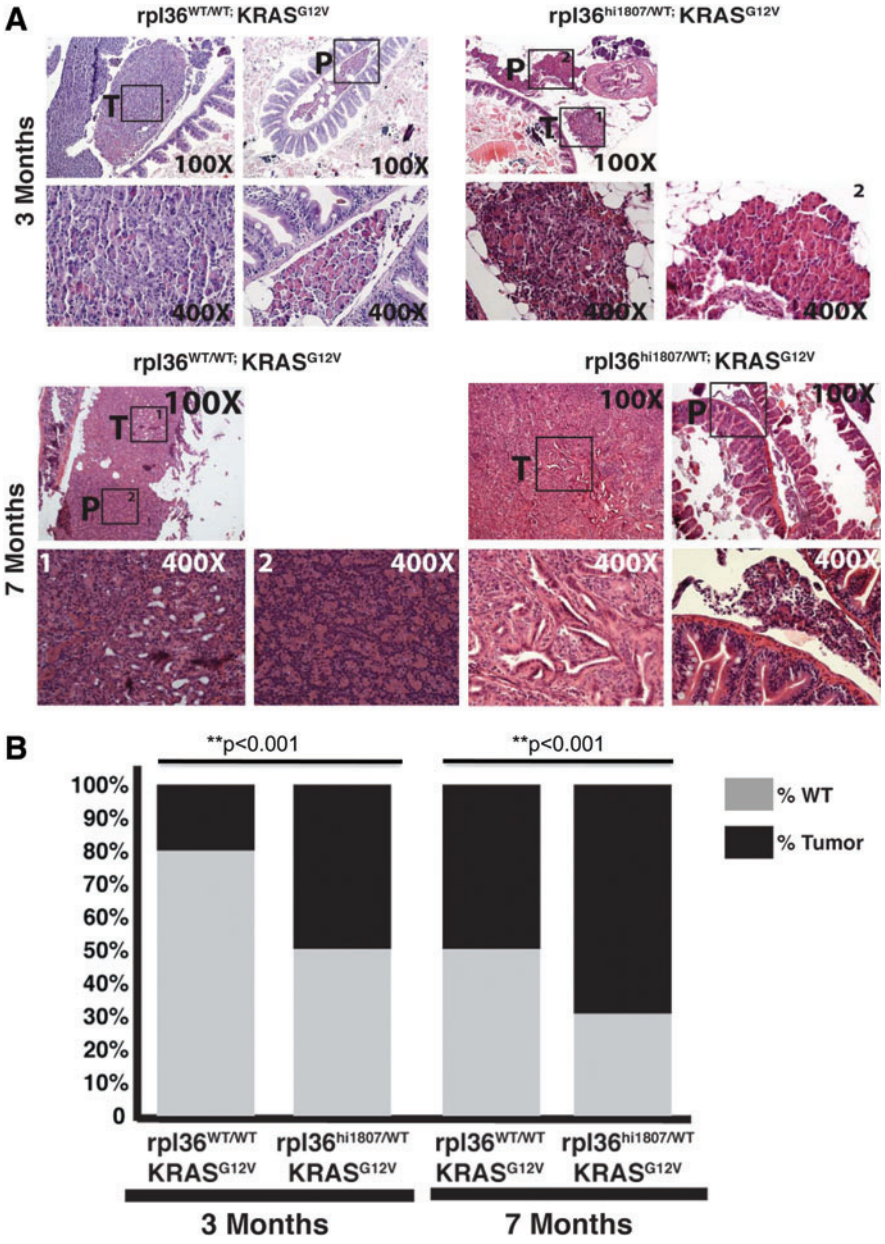

FIG. 3. Loss of *rpl36* increases the percentage of transgenic zebrafish with pancreatic tumors. **(A)** Histological analysis of tumors derived from KG^{ptf1a}; rpl36$^{+/+}$ or KG^{ptf1a}; rpl36$^{hi1807/+}$ zebrafish at 3 or 7 months of age at the time of sacrifice. Histology of dissected viscera with both non-neoplastic pancreas (P) and tumor tissue (T) for both zebrafish genotypes is represented. No differences in tumor histology are observed in the presence or absence of rpl36 haploinsufficiency. **(B)** The percentage of fish with normal histological pancreas (*gray*) or tumor (*black*) in 3- and 7-month-old *rpl36*$^{hi1807/WT}$*;ptf1a:gal4-VP16;UAS:GFP-KRAS*^{G12V} fish and their *rpl36*$^{WT/WT}$*;ptf1a:gal4-VP16;UAS:GFP-KRAS*^{G12V} control siblings (**$p <$ 0.001). Color images available online at www.liebertpub.com/zeb

tumors earlier than their *rpl36*$^{+/+}$ siblings (Fig. 2A). In addition, the rate of tumor progression, defined by the time between tumor detection by transcutaneous fluorescence and required sacrifice, was shorter for KG^{ptf1a}; rpl36$^{hi1807/+}$ fish than for their KG^{ptf1a}; rpl36$^{+/+}$ siblings (Fig. 2B, C). *Rpl36* haploinsufficiency also adversely affected the overall survival of KG^{ptf1a}; rpl36$^{hi1807/+}$ fish (median survival = 5.5 months ± 0.72 months vs. 7.5 months ± 1.34 months; $^{**}p < 0.0005$) (Fig. 2B). Thus, loss of a single *rpl36* allele significantly accelerates the progression of *Kras*-mediated pancreatic neoplasia.

To exclude any bias in tumor detection by transcutaneous fluorescence and to further confirm an increased tumor incidence in KG^{ptf1a}; rpl36$^{hi1807/+}$ fish, we performed scheduled sacrifice of fish at 3 and 7 months of age, regardless of whether tumors were visible or not. The fish were sacrificed, the endoderm was examined, and the presence or absence of pancreatic tumor was assessed (Fig. 3A). Similar to our assessment of tumor incidence by transcutaneous fluorescence, KG^{ptf1a}; rpl36$^{hi1807/+}$ fish had an increased incidence of tumors at both 3 and 7 months of age (Fig. 3B).

rpl36 restrains Kras^{G12D}-mediated proliferation

Ribosomal proteins are involved in ribosome assembly, which is tightly linked to the cell cycle.[18] To determine whether *rpl36* haploinsufficiency altered cell cycle dynamics downstream of oncogenic Kras, we investigated changes in the proliferation status in *rpl36^{hi1807}* mutant pancreas. In order to focus on changes in proliferation that might influence both tumor progression and tumor initiation, we examined PCNA labeling in both established tumors and oncogenic *KRAS*-expressing acinar cells even before the onset of histological tumor formation. Using this approach, we detected similar high proliferation indices in the tumor compartment in both KG^{ptf1a}; rpl36$^{hi1807/+}$ and KG^{ptf1a}; rpl36$^{+/+}$ pancreas (Fig. 4A, B). However, in adjacent normal (non-neoplastic) tissue, a significant increase in cell proliferation was noted in the KG^{ptf1a}; rpl36$^{hi1807/+}$ pancreas compared with control KG^{ptf1a}; rpl36$^{+/+}$ pancreas (Fig. 4A, B). Identical patterns were observed in tissue collected at 7 months of age (Fig. 4B). Quantification of PCNA-positive nuclei in the fluorescent *GFP-KRAS^{G12V}* domain revealed a statistically significant increase in the percent of proliferative cells in KG^{ptf1a};

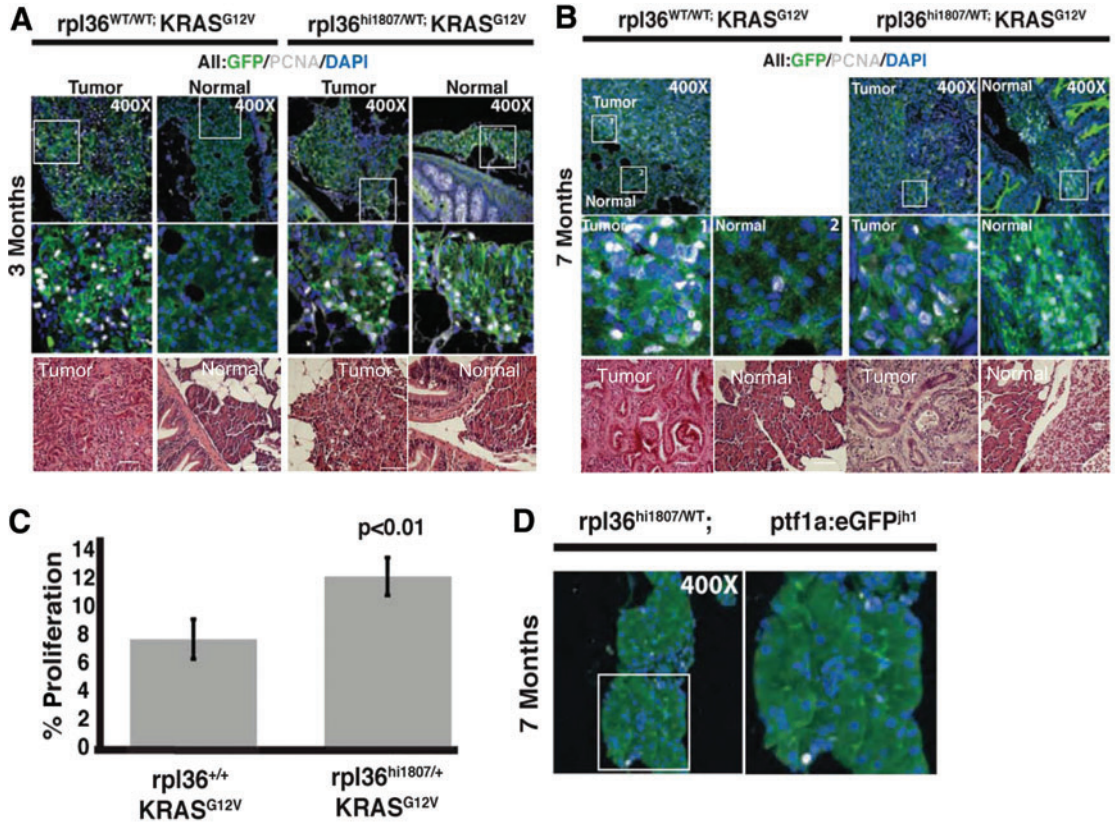

FIG. 4. Loss of rpl36 results in an increase in proliferation in ptf1a:gal4-VP16;UAS:GFP-KRAS^{G12V} pancreas. **(A, B)**, determination of cell proliferation using PCNA labeling (*white* nuclei) in tumor and normal pancreatic tissue harvested from control *rpl36$^{WT/WT}$;ptf1a:gal4-VP16;UAS:GFP-KRAS^{G12V}* and mutant *rpl36$^{hi1807/WT}$;ptf1a:gal4-VP16;UAS:GFP-KRAS^{G12V}* fish at 3 months **(A)** and 7 months **(B)** of age. Increased proliferation was detected only in tumor tissue harvested from *rpl36$^{WT/WT}$* fish, and not in adjacent normal tissue. In contrast, increased proliferation is seen in both tumor and adjacent normal tissue in *ptf1a:gal4-VP16;UAS:GFP-KRAS^{G12V}* fish with heterozygous *rpl36^{hi1807}* mutation **(C)**. Quantification of proliferative index of normal pancreatic tissue from control *rpl36$^{WT/WT}$;ptf1a:gal4-VP16;UAS:GFP-KRAS^{G12V}* and mutant *rpl36$^{hi1807/WT}$;ptf1a:gal4-VP16;UAS:GFP-KRAS^{G12V}* 3 month-old adult zebrafish. Students t-test, $^{**}p < 0.01$. **(D)** PCNA labeling of rpl36$^{hi1807/WT}$ zebrafish showing rpl36 haploinsufficiency does not increase proliferation in the absence of oncogenic KRAS. Color images available online at www.liebertpub.com/zeb

rpl36$^{hi1807/+}$ normal pancreas compared with control siblings (Fig. 4C).

Significantly, we did not see an increased proliferation index in G^{ptf1a}; rpl36$^{hi1807/+}$ heterozygotes in the absence of oncogenic *KRAS*^{G12V} (Fig. 4D). Rather, pancreatic tissue from these fish displayed a low frequency of PCNA labeling similar to that observed in the histologically normal pancreas of KG^{ptf1a}; rpl36$^{+/+}$ fish. These findings suggest that neither *rpl36* haploinsufficiency nor *KRAS*^{G12V} are individually capable of altering the proliferative state of the pancreas before histological tumor formation. However, in combination, they significantly increase proliferative rates in preneoplastic pancreatic epithelium, representing a possible mechanism for accelerated tumor initiation.

RPL36 protein levels are decreased in human and murine PanIN and pancreatic cancer

Our data showing that loss of one allele of *rpl36* promotes tumor formation suggest a tumor-suppressive role for rpl36 in the context of *KRAS*^{G12V}-mediated pancreatic cancer. In order to determine whether RPL36 might play a similar role in human pancreatic cancer, we mined previously published gene expression data.[19] These cDNA microarry experiments were performed on mRNA isolated from resected human pancreatic tissue, including bulk normal pancreas ($n=5$) and bulk PDAC ($n=17$), along with mRNA isolated from human pancreatic cancer cell lines. ONCOMINE data compiled from these cDNA arrays confirmed that *RPL36*, but not *RPL23a,* was downregulated in bulk human PDAC relative to normal pancreatic tissue (Fig. 5A, B). To determine whether RPL36 was expressed in human PanIN and invasive pancreatic cancer, we performed immunohistochemical labeling of RPL36 on mouse and human specimens. In non-neoplastic human pancreatic tissue, we observed moderate to high levels of *RPL36* expression in normal pancreatic epithelium, and a significant increase in areas of acinar-to-ductal metaplasia (ADM) arising in the setting of chronic pancreatitis. The intensity of RPL36 in human PanIN lesions was significantly reduced compared with the level observed in ADM (Fig. 5C,

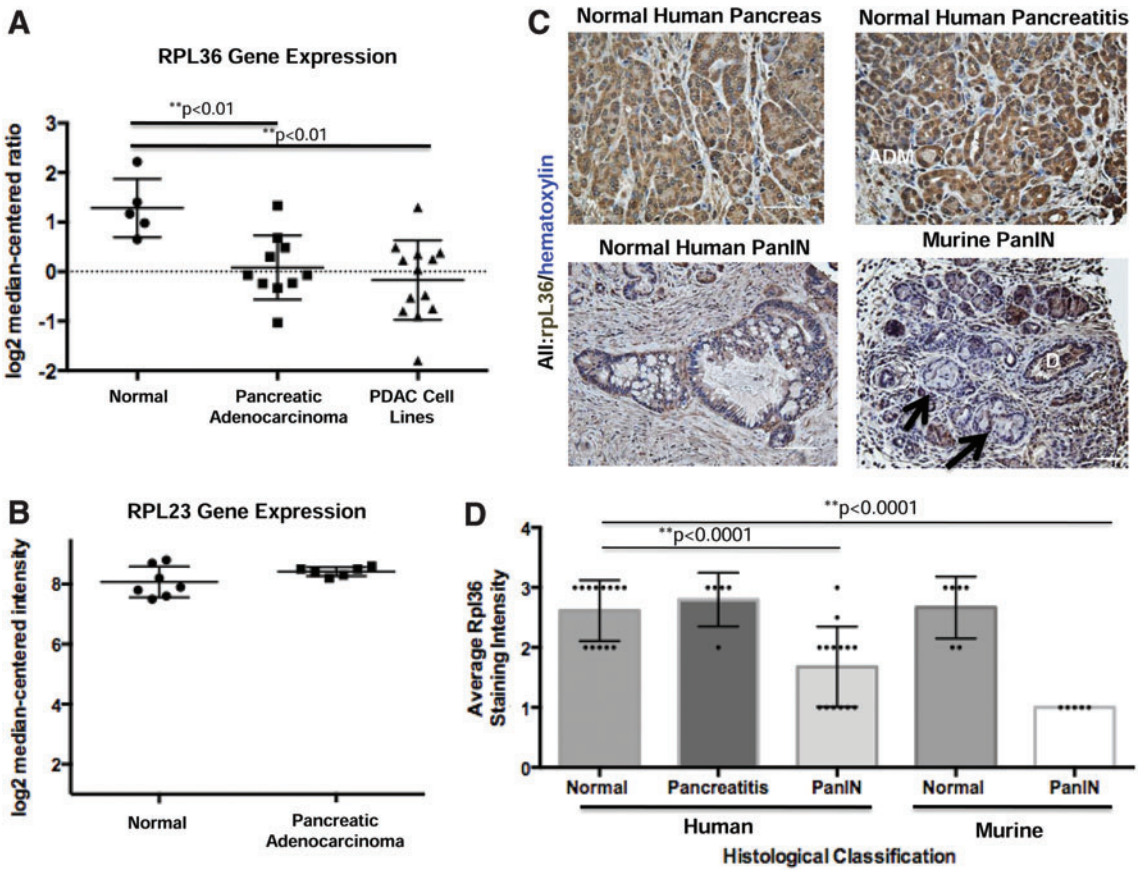

FIG. 5. Immunohistochemical analysis of RPL36 in human and murine pancreatic tissue. **(A, B)** Representative gene expression data for *RPL36* and *RPL23a.* (ONCOMINE). Microarray data confirm that *RPL36*, but not *RPL23a,* transcript abundance is decreased in bulk human pancreatic ductal adenocarcinoma specimens and in human PDAC cell lines relative to normal pancreas (data extracted from Iacobuzio-Donahue *et al.*, 2003). **(C)** Immunohistochemistry for RPL36. Analysis was performed on normal human pancreatic tissue, human chronic pancreatitis, and human PanIN. Immunohistochemistry was also performed on murine PanINs from *Mist1:CreER*^{T2}*;LSL-Kras*^{G12D} PanIN-bearing mice ($n=3$). Note high-level expression in normal pancreatic duct **(D)** but absent expression in PanIN lesions (*arrows*). **(D)** Graphical representation of average RPL36 staining intensity (1 = light staining; 3 = dark staining) as a function of pathological classification (n = minimum of 10 patient samples per group). RPL36 staining intensity was significantly decreased in human and murine PanIN relative to normal pancreatic tissue (**$p<0.0001$). Color images available online at www.liebertpub.com/zeb

D). Furthermore, murine PanIN lesions generated by the activation of oncogenic Kras in adult acinar cells exhibited a near absence of staining for RPL36, even while abundant staining was evident in adjacent acinar cells as well as in ducts not expressing oncogenic Kras (Fig. 5C). Combined with our functional evidence demonstrating that rpl36 restrains KRAS-induced pancreatic tumorigenesis in zebrafish, these data suggest that downregulation of RPL36 may also be required for PanIN initiation and/or progression in humans and mice.

To determine whether a similar reduction in rpl36 staining was observed in the zebrafish tumors, we selected a panel of tumors from the 3 and 7 month timepoints. Our analysis of rpl36 staining intensity indicated there was less pancreatic rpl36 staining in KG^{ptf1a}; $rpl36^{hi1807/+}$ zebrafish relative to the KG^{ptf1a}; $rpl36^{+/+}$ zebrafish (Fig. 6). In addition, we noted diminished rpl36 staining intensity in zebrafish pancreatic tumors when compared with normal zebrafish pancreas, similar to what we observed in murine and human PanIN. Among tumors arising in KG^{ptf1a};$rpl36^{hi1807/+}$ zebrafish, we saw variable levels of residual rpl36 expression by IHC, with some tumors retaining low level expression, and other tumors displaying minimal expression over background. These data suggest that a subset of tumors may undergo complete loss of rpl36 expression, potentially driven by loss of heterozygosity for the wild-type rpl36 allele, epigenetic silencing of the wild-type locus, or other post-transcriptional/post-translational mechanisms.

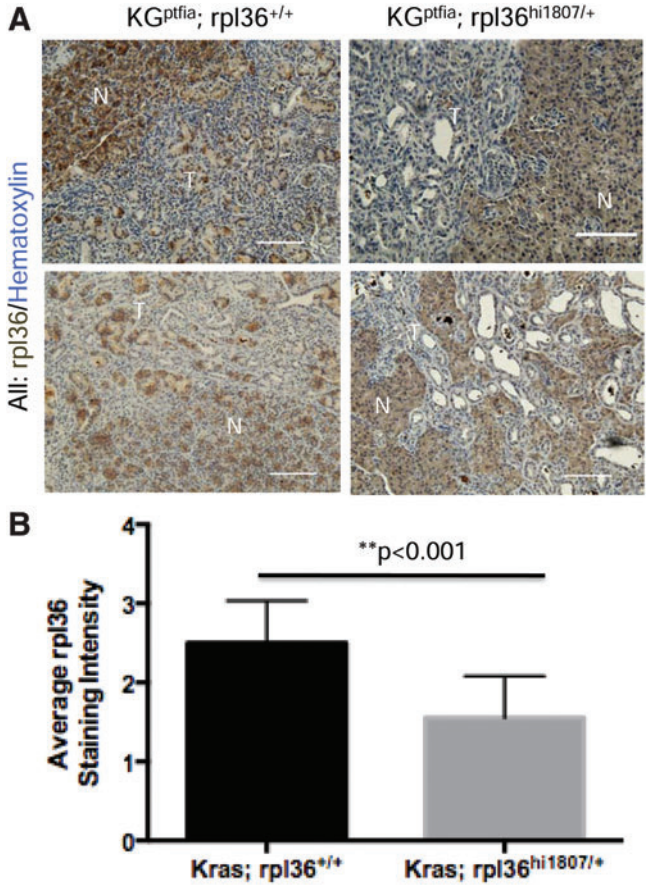

FIG. 6. Immunohistochemical analysis of zebrafish tumors reveals a significant reduction of rpl36 expression in KG^{ptf1a};$rpl36^{hi1807/+}$ tumors compared with KG^{ptf1a};$rpl36^{+/+}$ tumors. **(A)** IHC staining for rpl36 in a panel of tumor sections derived from either KG^{ptf1a}; $rpl36^{hi1807/+}$ or KG^{ptf1a}; $rpl36^{+/+}$ zebrafish ($n=8$ per group). **(B)** Quantification of staining intensity (1 = light brown staining, 3 = dark brown staining) in the tumor sections analyzed. Tumors occurring in fish with heterozygous loss of rpl36 displayed less intense labeling for rpl36. Color images available online at www.liebertpub.com/zeb

Discussion

In this article, we show that rpl36, but not rpl23, effectively restrains oncogenic Kras-induced pancreatic tumor formation in zebrafish. Haploinsufficiency for rpl36 enhances the proliferative response to oncogenic Kras in preneoplastic pancreatic epithelium, and leads to more rapid tumor progression and decreased survival. Corresponding to these observations in zebrafish, we have also documented decreased RPL36 expression in both preinvasive and invasive human pancreatic cancer, as well as in murine PanIN. Together, these studies suggest a conserved tumor suppressive role for rpl36 in vertebrate pancreas.

While the influence on rpl36 on pancreatic tumor progression seems clear, the precise mechanisms by which rpl36 haploinsufficiency in zebrafish or RPL36/Rpl36 downregulation in mammalian PanIN facilitates tumor progression remain to be determined. In addition to cooperating with oncogenic KRAS to accelerate pancreatic epithelial proliferation, another potential influence of rpl36 may be related to the regulation of pancreatic epithelial differentiation. Recent evidence suggests that pancreatic acinar cells represent an effective cell of origin for pancreatic ''ductal'' neoplasia in mice.[20–22] Pancreatic acinar cells are also known to express high levels of ribosomal proteins, reflecting their highly specialized capacity for digestive enzyme synthesis and secretion. In addition to cooperating with oncogenic KRAS to induce proliferation in normal acinar cells, haploinsufficiency for rpl36 may promote pancreatic tumor formation by promoting loss of the differentiated acinar cell phenotype. In this regard, a role for rpl36 in enforcing a differentiated acinar cell phenotype would be similar to the influence exerted by Mist1.[23]

In addition to multiple possible mechanisms by which rpl36 may restrain pancreatic tumor initiation and progression, the degree to which the tumor restraining function of rpl36 reflects a ribosomal or extra-ribosomal function for this gene product also remains uncertain. While rpl gene products are essential for proper assembly of the 60S subunit of the eukaryotic ribosome, many are also known to carry out additional extra-ribosomal functions, including DNA repair, transcriptional termination, cell cycle control, and leukocyte infiltration.[24–28]

In summary, we define a novel tumor-suppressive role for rpl36 in KRAS-mediated zebrafish pancreatic tumorigenesis, and demonstrate correlative changes in the expression of mammalian orthologues in the murine and human forms of this disease. These findings are consistent with the prominent role of ribosomes in pancreatic acinar cell biology, and underscore the fact that molecular events observed in human cancer should be considered in a specific cell and tissue

context. In addition, our findings further suggest that the neoplastic conversion of different cell types may be subject to different forms of genetic and epigenetic restraint.

Acknowledgments

This work was supported by NIH grants P01CA134292 and R01DK076233-01, as well as by an additional grant from the Lustgarten Foundation. SDL was also supported by the Paul K. Neumann Professorship in Pancreatic Cancer at Johns Hopkins University. JMB is supported by the PANCAN-AACR Pathway to Leadership Award and F32CA157044.

Disclosure Statement

No competing financial interests exist.

References

1. Feldmann G, Beaty R, Hruban RH, Maitra, A. Molecular genetics of pancreatic intraepithelial neoplasia. J Hepatobiliary Pancreat Surg 2007;14:224–232.
2. Corbo V, Tortora G, Scarpa A. Molecular pathology of pancreatic cancer: from bench-to-bedside translation. Curr Drug Targets 13:744–752.
3. Provost E, *et al.* Ribosomal biogenesis genes play an essential and p53-independent role in zebrafish pancreas development. Development 139:3232–3241.
4. Amsterdam A, *et al.* A large-scale insertional mutagenesis screen in zebrafish. Genes Dev 1999;13:2713–2724.
5. Amsterdam A, *et al.* Many ribosomal protein genes are cancer genes in zebrafish. PLoS Biol 2004;2:E139.
6. Lai K, *et al.* Many ribosomal protein mutations are associated with growth impairment and tumor predisposition in zebrafish. Dev Dyn 2009;238:76–85.
7. Zhang Y, *et al.* Inhibition of the p53-MDM2 interaction by adenovirus delivery of ribosomal protein L23 stabilizes p53 and induces cell cycle arrest and apoptosis in gastric cancer. J Gene Med 12:147–156.
8. Shen DW, Liang XJ, Suzuki T, Gottesman MM. Identification by functional cloning from a retroviral cDNA library of cDNAs for ribosomal protein L36 and the 10-kDa heat shock protein that confer cisplatin resistance. Mol Pharmacol 2006;69:1383–1388.
9. Khalaileh A, *et al.* Phosphorylation of ribosomal protein S6 attenuates DNA damage and tumor suppression during development of pancreatic cancer. Cancer Res 73:1811–1820.
10. Park SW, *et al.* Oncogenic KRAS induces progenitor cell expansion and malignant transformation in zebrafish exocrine pancreas. Gastroenterology 2008;134:2080–2090.
11. Pisharath, H, Parsons MJ. Nitroreductase-mediated cell ablation in transgenic zebrafish embryos. Methods Mol Biol 2009;546:133–143.
12. Godinho L, *et al.* Nonapical symmetric divisions underlie horizontal cell layer formation in the developing retina *in vivo*. Neuron 2007;56:597–603.
13. Pisharath H, Rhee JM, Swanson MA, Leach SD, Parsons MJ. Targeted ablation of beta cells in the embryonic zebrafish pancreas using *E. coli* nitroreductase. Mech Dev 2007;124:218–229.
14. Jones S, *et al.* Core signaling pathways in human pancreatic cancers revealed by global genomic analyses. Science 2008;321:1801–1806.
15. Liu S, Leach SD. Screening pancreatic oncogenes in zebrafish using the Gal4/UAS system. Methods Cell Biol 105: 367–381.
16. Davison JM, *et al.* Transactivation from Gal4-VP16 transgenic insertions for tissue-specific cell labeling and ablation in zebrafish. Dev Biol 2007;304: 811–824.
17. Halpern ME, *et al.* Gal4/UAS transgenic tools and their application to zebrafish. Zebrafish 2008;5:97–110.
18. Teng T Thomas G, Mercer CA. Growth control and ribosomopathies. Curr Opin Genet Dev 23:63–71.
19. Iacobuzio-Donahue CA, *et al.* Exploration of global gene expression patterns in pancreatic adenocarcinoma using cDNA microarrays. Am J Pathol 2003;162:1151–1162.
20. Kopp JL, *et al.* Identification of Sox9-dependent acinar-to-ductal reprogramming as the principal mechanism for initiation of pancreatic ductal adenocarcinoma. Cancer Cell 22:737–750.
21. Habbe N, *et al.* Spontaneous induction of murine pancreatic intraepithelial neoplasia (mPanIN) by acinar cell targeting of oncogenic Kras in adult mice. Proc Natl Acad Sci U S A 2008;105:18913–18918.
22. Guerra C, *et al.* Pancreatitis-induced inflammation contributes to pancreatic cancer by inhibiting oncogene-induced senescence. Cancer Cell 19:728–739.
23. Shi G, *et al.* Maintenance of acinar cell organization is critical to preventing Kras-induced acinar-ductal metaplasia. Oncogene 32:1950–1958.
24. Warner JR, McIntosh KB. How common are extraribosomal functions of ribosomal proteins? Mol Cell 2009; 34:3–11.
25. Kim TS, Kim HD, Kim J. PKCdelta-dependent functional switch of rpS3 between translation and DNA repair. Biochim Biophys Acta 2009;1793:395–405.
26. Torres M, Condon C, Balada JM, Squires C, Squires CL. Ribosomal protein S4 is a transcription factor with properties remarkably similar to NusA, a protein involved in both non-ribosomal and ribosomal RNA antitermination. EMBO J 2001;20:3811–3820.
27. Nishiura H, Zhao R, Yamamoto T. The role of the ribosomal protein S19 C-terminus in altering the chemotaxis of leucocytes by causing functional differences in the C5a receptor response. J Biochem 2011;150:271–277.
28. Bhavsar RB, Makley LN, Tsonis PA. The other lives of ribosomal proteins. Hum Genomics 2010;4:327–344.

Address correspondence to:
Steven D. Leach, MD
David M. Rubenstein Center
for Pancreatic Cancer Research
Memorial-Sloan Kettering Cancer Center
1275 York Avenue, Box 20
New York, NY 10065

E-mail: leachs@mskcc.org